


Shared optical parametric generation interactions in square lattice nonlinear photonic crystals

H. Chikh-Touami^{1,2}  · R. Kremer³ · H.-J. Lee⁴ · M. W. Lee¹ · L.-H. Peng⁴ · A. Boudrioua¹

Received: 13 September 2016 / Accepted: 15 March 2017 / Published online: 27 March 2017
© Springer-Verlag Berlin Heidelberg 2017

Abstract In this work, we investigated common optical parametric generation (OPG) with a 532-nm beam pumped along the x-axis of a square lattice two-dimensional periodically poled lithium tantalate (2D-PPLT). Twin-beam generation are observed with either the signal or the idler beams propagating collinearly to the pump beam due to participation of reciprocal lattice vectors (RLV) of $\mathbf{K}_{1,\pm 1}$. With both of the signal and the idler beams generated non-collinearly to the pump beam, multi-wavelength dual-beam generation are also observed due to contribution from $\mathbf{K}_{1,0}$ and $\mathbf{K}_{1,\pm 1}$. Because of mirror symmetry in the domain patterns/structures of the 2D-PPLT, all the OPG processes are doubled with the generated waves spectrally degenerated and spatially separated. By analyzing the spectral and angular distribution of the OPG beams, we confirm that the angular crossing of the $\mathbf{K}_{m,n}$ -assisted quasi-phase matching (QPM) spectral tuning curves result in a shared signal or idler wave configuration which leads to intensity enhancement in these parametric beams.

1 Introduction

In recent years, optical parametric generation (OPG) in second-order $\chi^{(2)}$ nonlinear photonic crystal (NLPC) has been the focus of research in nonlinear optics [1, 2]. It has been demonstrated that NLPC can be used for several applications, including multiwavelength generation [3], tunable infrared light sources [4, 5] and quantum optics [6], thanks to the flexibility offered by the existence of several reciprocal lattice vectors (RLV) due to the two dimensions of the lattice periodicity. Moreover, NLPC lattice can be one of the five possible Bravais gratings with different shape of the domain motifs offering more flexibility and several RLV to contribute to the same OPG processes. This can lead to further engineering in the nonlinear optical susceptibility tensor to activate parametric processes by means of designated Fourier components, i.e., $\chi^{(2)}(\mathbf{K}_{m,n}) \neq 0$. Experimental study demonstrated multiple and simultaneous wavelength generation due to the contribution of different RLV in 2D-PPLT crystal [7]. Multi-resonant optical parametric oscillator was also achieved by studying the generation efficiency and multi-wavelength generation in 2D-PPLT [8].

In fact, parametric optical interactions can be configured in such a way that the signal and idler waves exhibit large spectral bandwidths [9]; i.e., numerous signal and idler pairs at different frequencies can be generated during the same OPG process. A slight change in the propagation directions of the signal and idler waves might change the interaction geometry and thus permit different wave vectors to be involved in the quasi-phase matching (QPM)-processes by invoking proper reciprocal lattice vectors $\mathbf{K}_{m,n}$ to fulfill the law of momentum conservation. This could result in the concurrence of different frequency pairs for the QPM-OPG nonlinear processes which in turn,

✉ H. Chikh-Touami
hocine.chikh-touami@univ-paris13.fr

¹ Université Paris 13, Sorbonne Paris Cité, Laboratoire de Physique des Lasers, CNRS(UMR7538), 93430 Villetaneuse, France

² Ecole Militaire Polytechnique, UER Electronique, Laboratoire des Systèmes Electroniques et Optroniques, BP17 Bordj Elbahri, 16111 Algiers, Algeria

³ Université de Lorraine, Laboratoire Matériaux Optiques, Photoniques et Systèmes, EA 4423 Metz, France

⁴ Graduate Institute of Photonics and Optoelectronics and Department of Electrical Engineering, National Taiwan University, Taipei 106, Taiwan

substantially, enhance the overall conversion compared to 1D-NLPC [4, 6].

More recently, unique features of OPG interactions involved the use of either a shared signal or a shared idler wave in the QPM [9, 10]. These are coupled OPG which demands concurrence of two QPM processes activated by different RLVs with the idler or the signal wave generation to be spectrally and spatially degenerated. However, these studies mainly concerned on 2D NLPCs of hexagonal lattices. For instance, it has been reported on hexagonal 2D PPLT with a use of shared idler wave to give arise to a unique regime of OPG where a dual signal beam can be generated [1]. The authors also investigated the influence of the input angle dependence of the pump beam on the obtained shared signal and shared idler. Concurrent dual OPG processes have been also studied in Hex 2D PPLT demonstrating a coherent enhancement when two OPG processes share a common parametric beam [11].

In this work, we report the investigation of OPG interactions with a common parametric beam using a square lattice of 2D periodically poled LiTaO₃ (PPLT) and a pump beam at 532 nm propagating parallel to the symmetrical x-axis of the structure. We study coupled OPG necessitating two or more simultaneous processes phase matched by the same RLVs. Because of mirror symmetry (C2v), all the OPG processes are doubled with the generated waves spectrally degenerated and spatially separated. In particular, we, experimentally, study shared signal and shared idler interactions where unique features of the generated beams can be provided and controlled. By analyzing the spectral and angular properties of the output beams, we experimentally and numerically identify the contributions involved in the OPG processes. Our study might be of great interest for developing compact multipairs of entangled photons for quantum optics and multi-channel sources for optical telecommunication applications.

2 Shared parametric interaction in square lattice 2D-NLPC

As it is well known, in NLPC a QPM parametric process would require that both of the energy and the momentum conservation laws should be simultaneously satisfied, as given by Eq. (1).

$$\begin{cases} \lambda_p^{-1} = \lambda_s^{-1} + \lambda_i^{-1} \\ \mathbf{k}_p = \mathbf{k}_s + \mathbf{k}_i + \mathbf{K}_{m,n} \end{cases} \quad (1)$$

where \mathbf{k}_j and λ_j ($j = p, s, i$) are wave vectors and wavelengths of the pump, the signal and the idler, respectively, and $\mathbf{K}_{m,n}$ is the reciprocal lattice vector (RLV) of the (m, n)th order associated with the 2D NLPC. Note that efficient energy

transfer is permitted if and only if the law of momentum conservation is fulfilled as indicated in Eq.1. Under such condition, strong depletion in the pump energy can occur to transfer the pump energy into the signal and idler beams. Let us, also, recall that in the OPG process, \mathbf{k}_p is the only parameter that can be beforehand adjusted. It is related to propagation direction of the pump beam with respect to the x-axis of the structure (Here, we consider a z-cut LiTaO₃ sample with a periodically poled of square lattice shape). However, for each RLV $\mathbf{K}_{m,n}$, one can, in principle, find out a continuous set of possible signal and idler of different wavelengths and propagation directions. Moreover, one can also modify the incidence angle of the pump beam to add an additional degree of freedom to the OPG interactions occurring in the sample. The pump power also plays an important role for interactions where high-order RLVs are involved.

By considering the general case where the pump wave vector \mathbf{k}_p propagates at an angle θ_p from the structure x-axis, the conditions of a quasi-collinear phase matching can be described by the following two equations [2]:

$$\begin{cases} k_p \cos(\theta_p) = k_s \cos(\theta_s) + k_i \cos(\theta_i) + K_{m,n} \cos(\theta_{m,n}) \\ k_p \sin(\theta_p) = k_s \sin(\theta_s) + k_i \sin(\theta_i) + K_{m,n} \sin(\theta_{m,n}) \end{cases} \quad (2)$$

The exit angle of signal beams is expressed as follows:

$$(\alpha^2 + \beta^2) \cos^2(\theta_s) + 2\alpha\gamma \cos(\theta_s) + \gamma^2 - \beta^2 = 0 \quad (3)$$

with

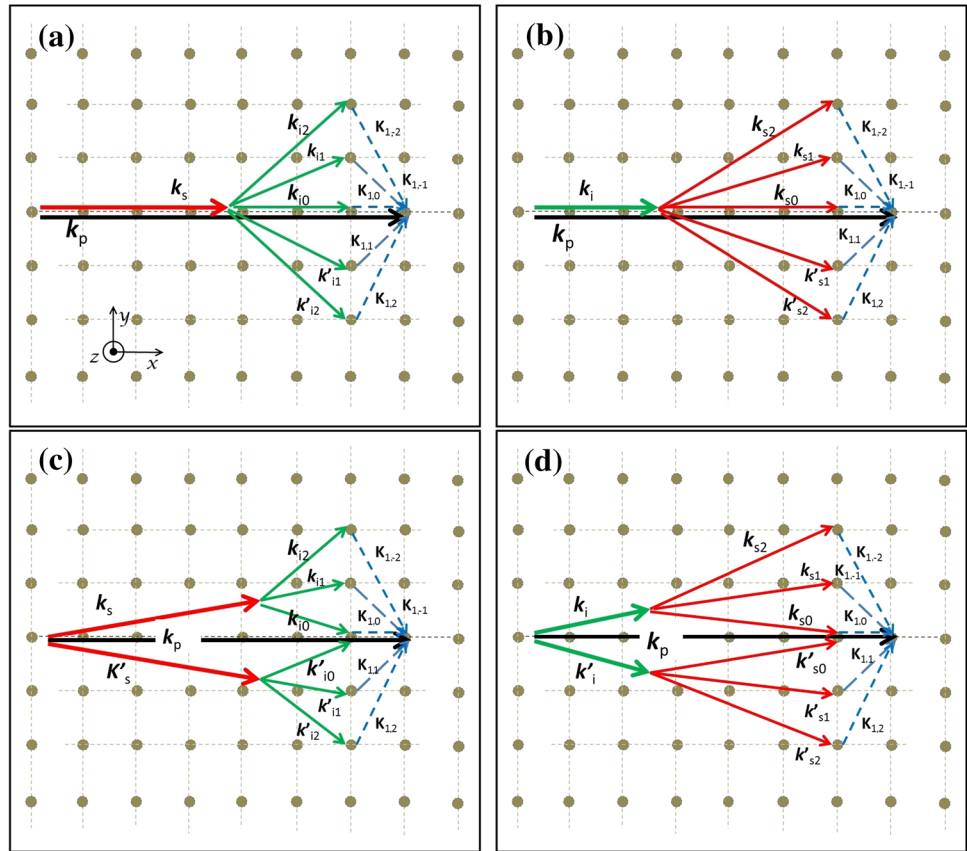
$$\begin{aligned} \alpha &= 2.k_s[K_{m,n} \cos(\theta_{m,n}) - k_p \cos(\theta_p)] \\ \beta &= 2.k_s[K_{m,n} \sin(\theta_{m,n}) - k_p \sin(\theta_p)] \\ \gamma &= k_p^2 - k_s^2 - k_i^2 + K_{m,n}^2 - 2k_p K_{m,n} \cos(\theta_p - \theta_{m,n}) \end{aligned}$$

Equations (2) and (3) are then used to calculate the spectral-angular tuning curves of different RLV $\mathbf{K}_{m,n}$ contributions as reported in many works.

As already indicated, in this work, we are, particularly, interested in studying the shared-signal OPG (SS-OPG) and the shared idler OPG (SI-OPG). To explore such possibilities, we schematically illustrate the geometric configuration in Fig. 1. Note that in Fig. 1a, c are shown the shared-signal OPG (SS-OPG) processes where \mathbf{k}_s is shared for multi-idler generation by various $\mathbf{K}_{m,n}$, whereas in Fig. 1b, d we illustrated the shared-idler OPG (SI-OPG) processes corresponding to a shared \mathbf{k}_i for multi-signal generation by various $\mathbf{K}_{m,n}$.

As it can be seen from Fig. 1, multi-wavelength generation due to concurrence of two $\mathbf{K}_{m,n}$ OPG processes becomes feasible. These beams present anti-correlation noise properties which can be used for quantum optics and optical telecommunications applications [12]. However, our study is restricted to the low-order RLV effect where OPG interactions are more

Fig. 1 QPM diagrams of shared signal OPG (SS-OPG) and shared idler OPG (SI-OPG) in square lattice 2D-NPC. **a**, **b** are for twin beam generation and **c**, **d** are for dual beam generation



significant. These low order of $\mathbf{K}_{m,n}$ have been calculated to support relatively high nonlinear gains [2] and with a domain duty cycle of 38% a high nonlinear optical conversion efficiency in a 2D NLPC can thus be expected [13]. Indeed the nonlinear susceptibility tensor arisen from a $\mathbf{K}_{m,n}$ -QPM process can be written as $\chi^{(2)}(\mathbf{K}_{m,n}) = d_{33} a_{m,n}$ where d_{33} and $a_{m,n}$ represent the nonlinear coefficient of material and the Fourier coefficient of $\mathbf{K}_{m,n}$, respectively. The optical parametric gain corresponding to SS (SI)-OPG configuration gain can be written as [2]:

$$g = \frac{2\mu_0\omega_s\omega_i|\mathbf{E}_p|}{\sqrt{\mathbf{k}_s\mathbf{k}_i}} \times d_{33}\sqrt{\sum |a_{m,n}|^2} \tag{4}$$

Note that a same signal (idler) wavelength can be generated in different output angle θ_s (θ_i) with different optical parametric gain. From Eq. (4) the effective nonlinear coefficient d_{eff} due to the crossing of two vectors $\mathbf{K}_{m,n}$ -assisted QPM processes can, therefore, be expressed as geometric sum of $a_{m,n}$, i.e.,

$$d_{\text{eff}} = d_{33}\sqrt{\sum |a_{m,n}|^2} \tag{5}$$

This effect can lead to gain enhancement in the angular-resolved OPG spectra due to crossing of the $\mathbf{K}_{m,n}$ -QPM processes in sharing the parametric beams.

3 Experiments

The 2D-PPLT sample (15 mm × 08 mm × 0.5 mm) used in our experiments was fabricated at room-temperature using the well-known electric-field poling technique [8]. The QPM-grating was square lattice with periods $\Lambda_x = \Lambda_y = 8.52 \mu\text{m}$, circular motif and a duty cycle of 38%. The choice of the lattice dimensions are connected to practical considerations as we used a pump beam at 532 nm to generate signal and idler in NIR region.

Our experimental setup is shown in Fig. 2. The pump source is a Q-switch Nd:YAG-doubled laser working at 532 nm, with a peak power pulse of 90 μJ , a pulse duration of 400 ps, and a repetition rate of 1 kHz. The pump beam is polarised along the z-axis of crystal to use its largest nonlinear coefficient d_{33} which leads to the type-0 nonlinear process $e \rightarrow e + e$. The crystal is mounted onto a temperature controller with a temperature setting of $T = 110^\circ\text{C}$ to avoid the photorefractive effect. Our pump laser was characterized with a quality factor $M^2 = 1.35$ and collimated inside the crystal with a waist radii of 350 μm and a Rayleigh range of 723 mm. The 2D PPLT crystal and the temperature control unit (oven) can rotate thanks to an accurate motor stage (with a resolution of 0.0005°). A long-wave pass filter with a cut-off wavelength at 650 nm (F) is used

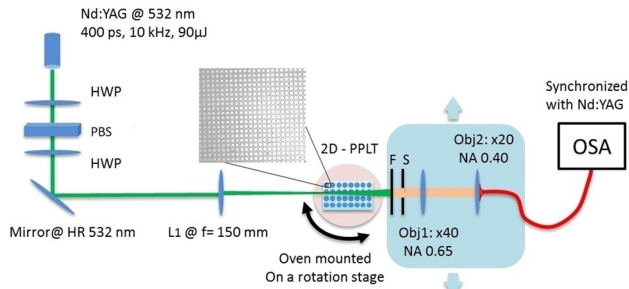


Fig. 2 Experimental setup used for the spectral-angular mapping of OPG. *Nd-YAG* Q switched laser, *HWP* half wave plate, *PBS* polarization beam splitter, *L1* and *L2* Lens, *F* long-wave pass filter @650 nm; *S* Pinhole; *Obj1,2* Microscopic Objective

to eliminate the pump beam after the crystal 2D-PPLT. A pinhole (*S*) in Fig. 2 acts as a spatial filter to eliminate the non-focus beams of objective *Obj1*. The generated OPG wavelengths are collected by objective *Obj2* and injected into an optical Spectrum Analyser (calibrated range from 350 to 1750 nm). The whole detection system (including the objectives, the filter, and the pinhole) is mounted on a translational stage which allows us to perform angle-resolved measurements of the OPG beams with respect to the symmetrical *x*-axis of the 2D PPLT crystal. By recording the beam spectra for every output angle θ_s (θ_i), we are able to complete the spectral-angular mapping of the OPG processes and compared the data with numerical calculation using Eqs. (2)–(3).

4 Results and discussion

It is worth noting that the threshold for observing OPG in our experiments was 15 MW/cm². In fact, we carefully consider the risk of damaging the PPLT crystal by choosing an appropriate crystal temperature (110 °C) to avoid the photorefractive effect. We also limited the injection pump intensity to be less than 25 MW/cm², which is well below an estimated damage threshold of 200 MW/cm² for the uncoated LiTaO₃ crystal. In fact, all the OPG processes have similar OPG threshold, as they appear simultaneously.

4.1 Collinear OPG: k_s and k_i parallel to k_p

The most familiar case of OPG in a 1D QPM structure is that k_p , k_s and k_i participating in the three-wave mixing process are all parallel (collinear) to each other. This kind of collinear QPM-OPG process can also be applied to the 2D square lattice PPLT with the contribution of the RLV $K_{1,0}$ at $\theta_p = \theta_s = \theta_i = 0$. The recorded spectra of OPG corresponding to the collinear configuration are

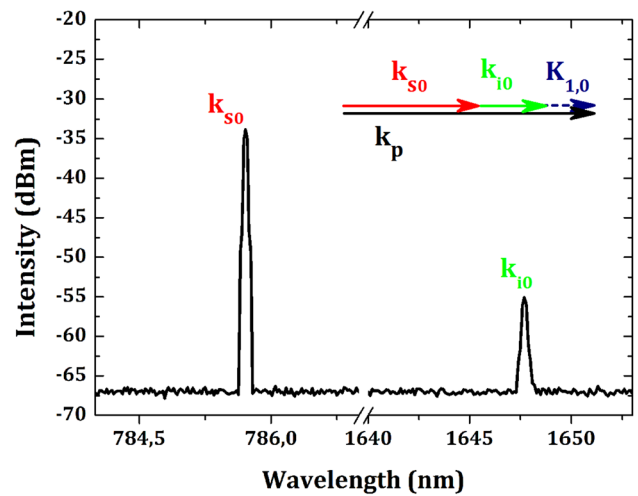


Fig. 3 Output signal and idler beams in collinear OPG process

illustrated in Fig. 3 with the signal and the idler detected at 785.86 nm and 1647.51 nm, respectively. The experimental data are analysed using simulations based on equations presented in the previous section. Note that, high-order RLV such as $K_{1,\pm 2}$ was difficult to record due to the spectral limitation of our OSA.

4.2 Twin-beam generation: either k_s or k_i parallel to k_p

In this configuration, symmetrically located lowest order RLV $K_{1,1}$ and $K_{1,-1}$ are concerned for the twin-OPG processes. Such paired RLVs owns equal amplitudes and are oriented at $\pm 45^\circ$ with respect to the propagation direction (*x*-axis of the structure) of the pump beam. This mechanism allows concurrence of twin-beam generation in Fig. 1a of shared signal optical parametric generation (SS-OPG) or Fig. 1b of shared idler optical parametric generation (SI-OPG). At a crystal temperature of 110°C, the SS-OPG processes are found to share a common signal beam at 743.4 nm which is collinear with the pump incident beam in Fig. 4a. Note that for this interaction we were not able to record the idler beam spectrum as it is situated at $\lambda_i = 1876.3$ nm which is out of the detection range of our measurement system. For the SI-OPG process, a common idler at 1736 nm also collinear with the pump beam is recorded in Fig. 4b. In addition, twin beam of coherent signals at 765.5 nm located at $\pm 2.38^\circ$ with respect to the *x*-axis were also recorded in Fig. 4b. It is worth noting that in this latter case, the signal has a lower intensity than that obtained in the SS-OPG process. This might be due to the large walk-off angle of $\pm 2.38^\circ$ between the pump and the signal beams.

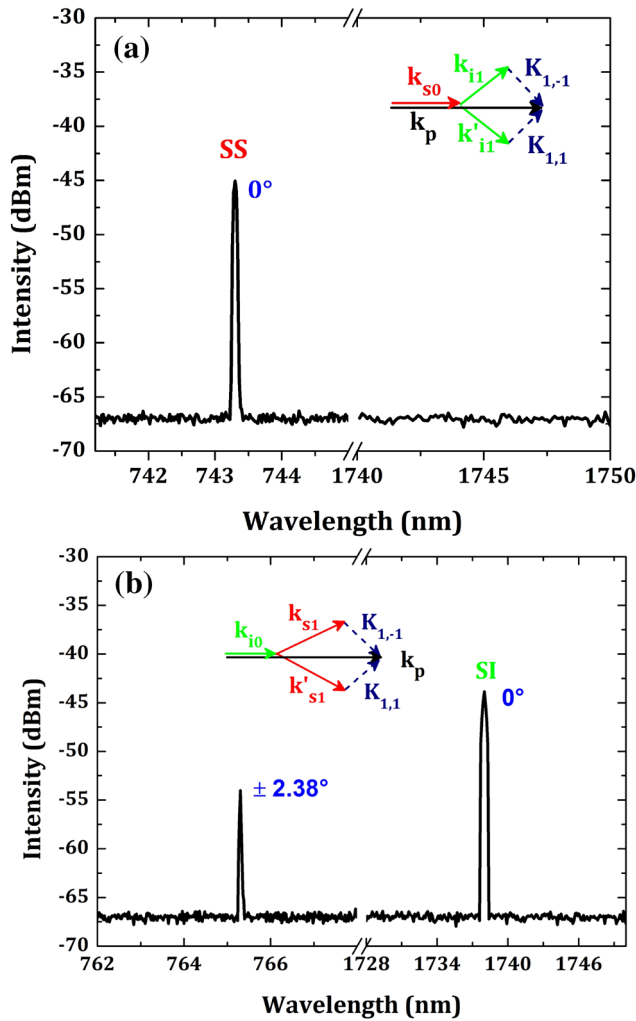


Fig. 4 Twin-beam generation processes. **a** Shared signal (SS-OPG). **b** Shared idler (SI-OPG)

4.3 Dual-beam generation: none of k_s and k_i parallel to k_p

In this configuration, $K_{1,0}$ and $K_{1,\pm 1}$ are involved in the SS-OPG and SI-OPG processes, ensuring the generation of a pair of idler (1711, 1727 nm) and signal (768 nm, 768.5 nm), respectively, and taking place simultaneously. In this QPM geometry none of the three interacting wave vectors of (k_s, k_i, k_p) are parallel to each other. Indeed, from the spectra recorded in Fig. 5a, contribution of $K_{1,0}$ and $K_{1,\pm 1}$ to the SS-OPG processes can be clearly resolved as follows. Namely, the signal beam, common to the aforementioned QPM processes, was recorded at $\pm 1.19^\circ$ at wavelength of 770.25 nm. In comparison, the idler beams were recorded at a much lower power, reached approximately 10 % of the signal beam and deflected at $\pm 2.86^\circ$ for $\lambda_i = 1727.9$ nm and at $\pm 1.66^\circ$

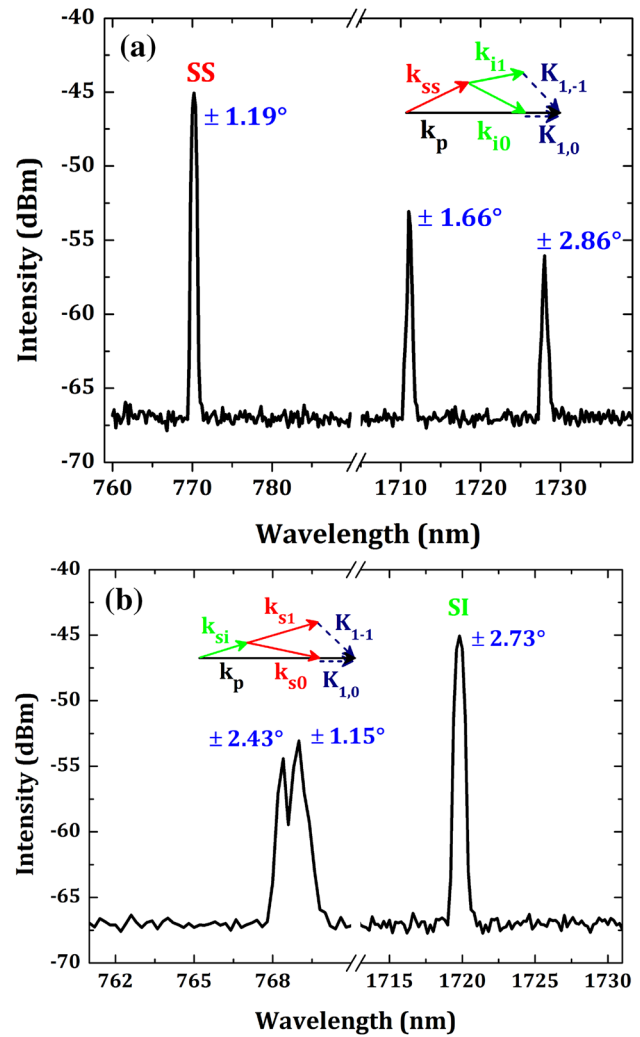


Fig. 5 Dual beam generation processes. **a** Shared signal (SS-OPG). **b** Shared idler (SI-OPG)

for $\lambda_i = 1711.4$ nm, corresponding to the $K_{1,0}$ and $K_{1,\pm 1}$ activated QPM-OPG, respectively.

Moreover, for the SI-OPG processes, the common idler beam of wavelength 1719.8 nm was detected at an off axis angle of $\pm 2.73^\circ$, while the two signal beams corresponding to the $K_{1,0}$ and $K_{1,\pm 1}$ activated QPM process were separately detected at $\pm 1.15^\circ$ and $\pm 2.43^\circ$ for wavelength 768.4 and 768 nm (Fig. 5b).

It should be noted that the spectra displayed in Fig. 5 were recorded on the positive side of the output angles and we have measured similar spectra in the other negative side of angles due to mirror symmetry. These observations reveal mirror reflection symmetry for a square 2D PPLT NLPC upon which the OPG processes were due to a pump beam propagating along the crystal's x-axis. By a simple geometrical analysis as it can be seen from Fig. 1, one can emphasize that idler beam at 2.86° was in fact the

mirror-symmetrical contribution of the same OPG interaction. The same analysis can be applied to the case of SI-OPG which indicates that the signal beam at 1.15° comes from the mirror-symmetrical contribution in the same interaction.

As a matter of fact, these unique OPG interactions where signal (idler) are shared to generate twin beams or dual beams can be easily identified from the intersection points of the curves reported in Fig. 6. These curves give the general behavior of the recorded signal and idler wavelengths as a function of the output angles (λ_s and λ_i , respectively). The simulation results are performed using Eqs. (3) and (4) and by taking into account the Sellmeier equation [5] and the experimental conditions such as the temperature for high conversion efficiency which is 110 °C [7]. Measurements are found with a very good agreement with simulations.

Experimentally, we found that the SS-OPG in square lattice 2D-PPLT processes are dominant as shown in

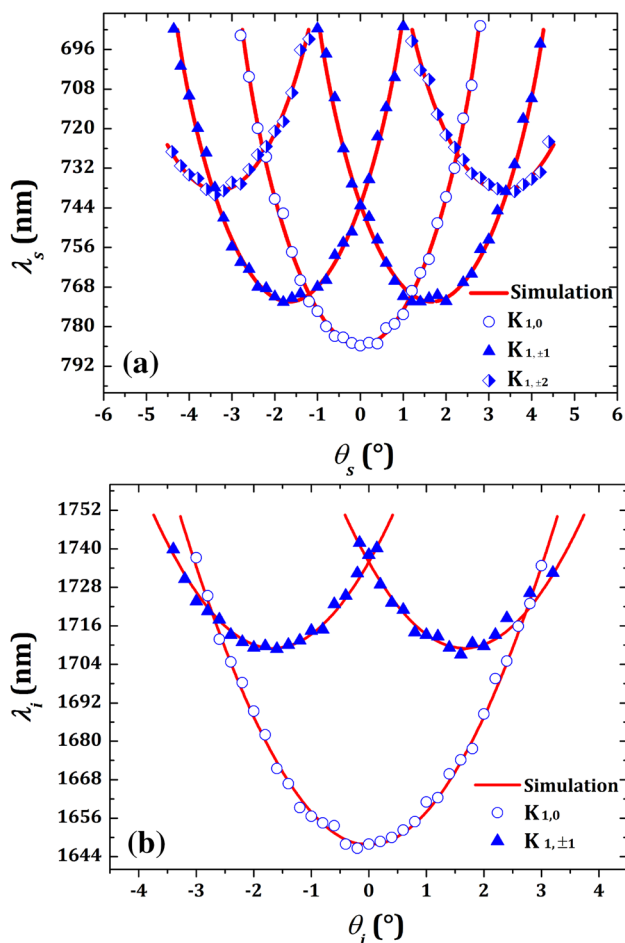


Fig. 6 Measured shared reciprocal vector (SRLV-OPG), shared signal (SS-OPG) and shared idler (SI-OPG) in square lattice 2D-PPLT crystal. **a** $K_{1,0}$, $K_{1,\pm 1}$ and $K_{1,\pm 2}$ for signal. **b** $K_{1,0}$ and $K_{1,\pm 1}$ for idler

Fig. 6. But the common-signal case corresponds to a larger noncollinear angle between the pump and idler beams, thus a shorter spatial walk-off length; therefore, the parametric gain will be lower compared with the common-idler case.

From these figures, it is interesting to underline the evolution of spatial form of parametric beams for a fixed signal or idler wavelength. The same wavelength can appear two-port output (at 780 nm), four-port output (at 770 nm), or even six-port output (at 756 nm), for instance. This might be of great interest for multichannel applications.

Ultimately, we have estimated the overall conversion efficiency for the studied OPG interactions to be about of 16%. This value is relatively large compared to those reported such as reference [11]. However, it is important to conduct a thorough investigation to measure experimentally the conversion efficiency of different processes and to determine the contribution of each RLV to the overall conversion efficiency. This might be a continuation of this work.

5 Conclusion

In this work, we have experimentally demonstrated the feasibility and the flexibility of common OPG interactions in square lattice 2D-PPLT crystal. We particularly focused on the case where the incident pump beam is parallel to the symmetrical axis of the structure. We, experimentally, studied shared signal and shared idler interactions where unique features of the generated beams can be provided and controlled. On the one hand, twin beams can be generated when symmetrically located lowest order RLV $K_{1,1}$ and $K_{1,-1}$ are concerned with the signal (idler) collinear to the pump beam. On the other hand, dual beams can be obtained when $K_{1,0}$ and $K_{1,\pm 1}$ are involved in the SS-OPG and SI-OPG processes with the signal (idler) noncollinear with the pump beam. Because of mirror symmetry, all the OPG processes are doubled with the generated waves spectrally degenerated and spatially separated. By mapping the spectral and angular properties of the output beams, we experimentally and numerically identify the contributions involved in the shared-OPG processes. The overall conversion efficiency is estimated to be about of 16%. A thorough investigation of the contribution of each RLV interaction to the overall conversion efficiency can allow us to manage the output signals for the application needed.

Acknowledgements The authors thank very much Mr. Billeton Thierry for the assistance in preparing the experiments. They also acknowledge the support of MOST 104-2221-E-002-071-MY3.

References

1. Martin Levenius, Valdas Pasiskevicius, Katia Gallo, *Appl. Phys. Lett.* **101**, 121114 (2012)
2. H.-C. Liu, A.H. Kung, *Opt. Exp.* **16**(13), 9714–9725 (2008)
3. W.K. Chang, Y.H. Chen, H.H. Chang, J.W. Chang, C.Y. Chen, Y.Y. Lin, Y.C. Huang, S.T. Lin, *Opt. Exp.* **19**(24), 23654–23651 (2008)
4. L.-H. Peng, C.-C. Hsu, J. Ng, A. H. Kung, *Appl. Phys. Letters* **84**, 3250 (2004)
5. J.-P. Meyn, M.M. Fejer, *Opt. Lett.* **22**(16), 1214–1216 (1997)
6. Y.-X. Gong, P. Xu, J. Shi, L. Chen, X. Q. Yu, P. Xue, S.N. Zhu, *Opt. Lett.* **37**(21), 4374–4376 (2012)
7. M. Lazoul, A. Boudrioua, L.M. Simohamed, A. Fischer, L.-H. Peng, *Opt. Lett.* **38**(19), 3892–3894 (2013)
8. M. Lazoul, A. Boudrioua, L.M. Simohamed, A. Fischer, L.H. Peng, *Opt. Lett.* **40**(8), 1861–1864 (2015)
9. M. Conforti, F. Baronio, M. Levenius, K. Gallo, *Opt. Lett.* **39**(12), 3457–3460 (2014)
10. H. Cankaya, A.-L. Calendron, H. Suchowski, F.X. Kärtner, *Opt. Lett.* **39**(10), 2912–2915 (2014)
11. L. Chen, P. Xu, Y.F. Bai, X.W. Luo, M.L. Zhong, M. Dai, M.H. Lu, S.N. Zhu, *Opt. Exp.* **22**(11), 13164–13169 (2008)
12. V. Berger, *Phys. Rev. Lett.* **81**, 4136 (1998)
13. A. Arie, N. Habshoosh, A. Bahabad, *Opt. Quant Electron* **39**, 361–375 (2007)